International Conference on Renewable Energies and Power Quality (ICREPQ'13)
Bilbao (Spain), 20th to 22th March, 2013
Renewable Energy and Power Quality Journal (RE&PQJ)
ISSN 2172-038 X, No.11, March 2013

Modelling and Design of Indirect Solar Dryers for Batch Drying

L. Blanco-Cano, A. Soria-Verdugo, L.M. Garcia-Gutierrez and U. Ruiz-Rivas

Department of Thermal and Fluids Engineering
E.P.S., Carlos III University of Madrid
Avda. Universidad 30, 28911 Leganés (Spain)
Phone/Fax number: +34 916 246034, e-mail: **lbcano@ing.uc3m.es**

Abstract. A model is developed to study the influence of design parameters (dimensions, air mass flow rate) in the performance of an indirect solar drier for batch drying. The aim of the work is to cover a wide range of configurations and sizes with a simple model. The model covers the air heating in the collector and the vapour mass transfer in the drying chamber. Constant rate controlled by convection mass transfer is assumed. The results, still preliminary, show the relevance of using a solar collector and the evolution of the drying process in the drying chamber. The obtainable vapour mass flow rate is calculated for a variety of configurations, showing the incidence of the air mass flow and the dimensions of the collector and the drying chamber. Performance parameters such as temperatures during the process and the efficiency of the drying chamber are also depicted.

Key words
Solar thermal, solar drying technology, dryer design, energy for developing regions.

1. Introduction

Postharvest losses in developing countries are estimated to be a 30% - 40% of the production [1]. Drying the products can reduce drastically these losses as a better preservation can be achieved. Heated air dryers use the water mass transfer between a product and an airflow. Air is heated to increase its capacity to absorb water vapour. Solar dryers for agricultural and forest products, in which the air is heated in a solar collector, has extended due to the rapid increase of the fossil fuels price. Besides, in rural impoverished areas, access to industry is not always guaranteed. It is important, hence, to develop well-designed and efficient solar dryers, economically and technologically feasible for this sector, to overcome the gap between rural and industrial producers.

A wide range of types of solar dryers exist. A first classification attends to the nature of motion of the airflow. This can be natural convection or forced convection by means of a fan. Besides, solar dryers can be classified into direct, indirect or mixed depending on the parts exposed to solar radiation. In direct solar dryers, the product is set in a chamber with a transparent wall, so solar radiation hits the product directly. Indirect solar dryers (Fig.1) have a solar collector where the airflow is heated before being drive into the opaque drying chamber. Mixed mode solar dryers combine both types, so solar radiation is absorbed both by the collector and the drying chamber.

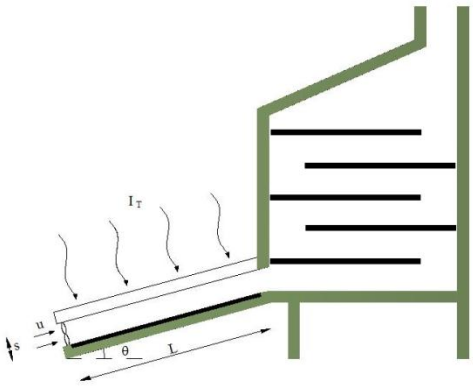

Fig.1: Scheme of a general solar dryer

This work presents a theoretical study on the drying capacity of an airflow for a wide range of design parameters, depending on the solar collector performance and the relation of the drying chamber and the collector geometrical parameters. The study considers indirect solar dryer, as the one shown in Fig.1. The product to be dried is set in batches along the trays of the drying chamber, and the air is forced to flow through the circuit.

2. Basic equations

The drying capacity of an airflow depends on its relative humidity and its mass flow rate. Thus, if the air is heated in a collector, the temperature increase yields a relative humidity decrement, and the mass flow rate of vapour that the airflow is capable of absorbing increases. Assuming steady state conditions, the temperature of the airflow leaving the solar collector depends on the solar irradiance over the collector area, the collector efficiency and the mass flow rate. This can be seen in the energy balance:

$$\dot{m}_a C_{p_a}(T_{c,out} - T_{c,in}) = \eta I_T A_c \quad (1)$$

The efficiency of the solar collector is expressed as [2]:

$$\eta = F_R\tau\alpha - F_R U_L \frac{T_{c,out}-T_{c,in}}{I_T} \quad (2)$$

The heat removal factor F_R, relates the actual heat gain to the heat gain that would result if the absorber was at the temperature of the airflow at the outlet of the collector. It depends on the type of collector and the mass flow rate, and it has to be experimentally determined. For simplicity, F_R is assumed constant in the present work, this is, independent from $\dot{m}_a$. U_L can also be assumed constant [2]. The optical properties, transmittance τ and absorptance α, depend on the materials of both the cover and the absorber. However, as the aim of this paper is to scope a wide range of types of solar dryers, overall values based on literature have been taken for these parameters and assumed constant in the whole process. Therefore, combining eq.1 and eq.2:

$$T_{c,out} = T_{c,in} + \frac{F_R\tau\alpha}{\frac{C_{pa}\dot{m}_a}{I_T A_c} + \frac{F_R U_L}{I_T}} \quad (3)$$

As the variation of temperature within the working range is too small, the air density and specific heat are assumed constant. No water is added or extracted during the heating process, so specific humidity remains constant during this process. As it can be seen in Fig.1, the air leaving the collector is driven to the drying chamber, where the drying process occurs. The drying process is assumed to be adiabatic (and thus isenthalpic for the airflow). The drying process can be modeled using psychrometric equations. The saturation conditions of the airflow leaving the drying chamber will be those obtained from solving the equation system (4):

$$\omega_{o,sat} = \frac{C_{p_a}(T_{c,out}-T_0)+\omega_{in}\left(h_g+Cp_v(T_{c,out}-T_0)\right)}{h_g+C_{pv}(T_{o,sat}-T_0)}$$
$$T_{o,sat} = \left(\frac{1}{T_{ref}} - \frac{R_g}{h_{fg}}\mathrm{Ln}\left(\frac{\omega_{o,sat}}{(0.622+\omega_{o,sat})}\frac{P_{atm}}{P_{ref}}\right)\right)^{-1} \quad (4)$$

The sub-index *sat* denotes that the air leaving the chamber is saturated. This will lead to a maximum drying effect in the chamber (as for an infinite chamber). Saturation is thus, a limit condition that would be reached or not depending on the dynamics of the process. It represents an upper limit for the process and corresponds to the case in which maximum mass flow of vapour is transferred.

The maximum mass flow of vapour that can be absorbed by the airflow is then calculated. It represents the drying capacity, and it is obtained as the product of air mass flow and the specific humidity difference between ambient conditions and saturation, calculated solving the equation system 4 as a function of the presented parameters.

$$\dot{m}_v = \dot{m}_a(\omega_{o,sat} - \omega_{c,in}) \quad (5)$$

In order to see the energy needed to vaporize the water, drying capacity should be multiplied by the enthalpy of evaporation h_{fg}. Results are adimensionalized by means of the total solar power entering the collector:

$$\overline{\dot{m}_v} = \frac{\dot{m}_v h_{fg}}{I_T A_c} \quad (6)$$

The drying process along the drying chamber has been studied in order to establish how that maximum could be reached. The drying process can either be controlled by the mass transfer from the surface or by unsaturated surface and internal moisture motion mechanisms. In the first case, a sufficient water supply to the surface from the internal structure of the drying material is assumed, so the process will be controlled by the mass convection rate from the surface to the airflow. In the second case, the process dynamics is controlled by the diffusion rate of internal moisture to the suface. This study will focus on the first case: mass transfer process controlled by the mass convection rate. The vapour mass flow is given by:

$$\dot{m}_v = KA_d(\omega_{sat} - \omega_\infty) \quad (7)$$

K represents the convective mass transfer coefficient. A_d is the drying surface, ω_{sat} is the specific humidity for saturation conditions at the surface temperature, and ω_∞ is the specific humidity of the airflow. The surface temperature T_s is obtained from the energy balance in the surface (here, given in a simplified form, neglecting conduction and radiation terms). Steady state is assumed:

$$h_c(T_\infty - T_s) = K(\omega_{sat} - \omega_\infty)h_{fg} \quad (8)$$

Mass and heat convection coefficients in eq.8 can be calculated for turbulent flow using equation 9 [3].

$$\frac{h_c}{C_{p_a}\rho u}\mathrm{Pr}^{2/3} = \frac{K}{\rho u}\mathrm{Sc}^{2/3} = 0.11\mathrm{Re}_D^{-0.29} \quad (9)$$

Where Re_D is the Reynolds number referred to the hydraulic diameter of the cross-section. Eq.8 is only valid for internal turbulent flow ($2600 < Re_D < 22000$). The evolution of the temperature of the airflow T_∞ and the temperature of the drying surface T_s along the length of the drying chamber can be now determined.

3. Numerical procedure and input data

A numerical procedure was established using MatLab™. The problem was divided in two parts: an analysis of the collector performance, and an analysis of the drying process taking place in the drying chamber. The first one gives the drying capacity of the system, while the second one studies the incidence on the process of the drying chamber dimensions and arrangement. The results, still preliminary, can be used to study the interactions between collector and drying chamber in order to define design criteria. Steady state conditions were considered.

The collector performance was analysed in terms of the temperature that the airflow can reach and the collector efficiency. Varying parameters are the collector dimensions and the air mass flow rate. Aggregating the relevant parameters, a single variable was used. This variable is the mass flow rate per unit of collector area $\dot{m}_a/A_c$. For the present results ambient conditions are set to be 25ºC, 70% relative humidity and a solar irradiance of 800W/m^2, which represent average tropical conditions. Once the collector performance is studied, the maximum obtainable drying capacity of the airflow can be calculated as a function of $\dot{m}_a/A_c$.

The drying chamber performance is analysed using a numerical method in an upwind scheme. The length of the drying path is discretized into differential elements (N~10^3). In each element, the air and surface average temperatures are calculated using an iterative method based on eq.8 and the energy balance. The initial guess is the air temperature at the inlet of the element (inlet of the drying chamber for the first element). With that temperature, T_s is calculated from eq.8 for the first element. Then, the air temperature leaving the differential element is calculated using an energy balance and the average air temperature is set. Eventually, the average surface temperature must be readjusted. Once the process converges, it is repeated in the next differential element following an upwind scheme along the drying path, and thus the temperature distributions of the airflow and the surface are obtained.

The range of variation of the key parameters ought to be established, and some are given a fixed value for this preliminary work. An investigation in literature was done in search of the common working range. The general zone of interest of $\dot{m}_a/A_c$ for indirect solar dryers is in the 10^{-3} to 10^{-1} kg/(s·m^2) range (see, for example [4]-[7]). This is the only parameter (apart from ambient conditions established above) affecting the collector calculations. For the drying chamber calculations, other restrictions are necessary. Some geometrical parameters in both collector and drying chamber ought to be set to obtain the airflow velocity in the drying chamber. Then, the interval of $\dot{m}_a/A_c$ should be set to cope the restrictions of eq.9. Conditions for the drying chamber calculations are then as follows: collector length, L, is set to 1m., collector and drying chamber airflow cross sections (between trays) are the same ($W = W_d$ and $s = s_d = 0.1$m). Therefore, air velocities are varied between 0.2m/s and 1.7m/s, and $\dot{m}_a/A_c$ ranges between 0.02 kg/(s·m^2) and 0.17 kg/(s·m^2) . This range fits the upper part of the working range found in literature used in the collector calculations. In order to fit the lower range, mostly designated for natural flow applications, a natural flow correlation for the mass and heat flow should be used.

4. Results

In this section, the results of the calculations for the drying capacity of the airflow are presented. In the first sub-section, the collector performance is analysed in terms of the outlet temperature and the maximum vapour mass flow. In the second one, the drying chamber performance is analysed.

A. Collector performance

The air enters the solar collector at ambient conditions and is heated. The air leaving the collector is immediately driven into the drying chamber. The temperature at the outlet of the collector / inlet of the drying chamber, calculated using eq.3, is shown in Fig.2. It is a function of the air mass flow rate per unit of collector area. Solar irradiation has a linear effect on the temperature increase in the collector as shown in eq.3. Therefore, changes on the solar irradiance yield linear variations in the presented temperature.

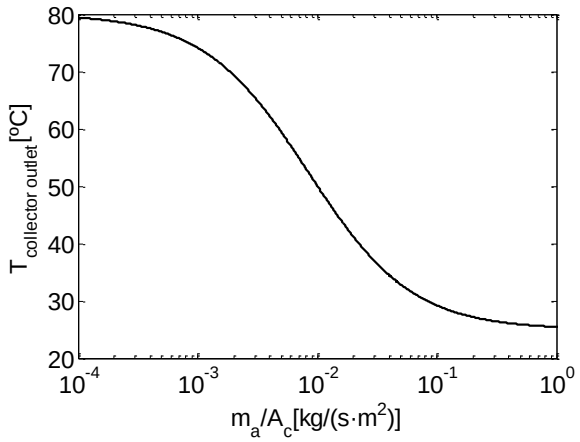

Fig.2. Temperature at the collector outlet

Fig.2 shows results for a wide range of mass flows and collector areas, consequent with the range previously selected. Three characteristic zones are present. For low mass flows per unit collector area, a maximum temperature is approached, due to two competing mechanism: a large temperature increase due to the low mass flow per unit of heat transfer and a low efficiency on the collector due to high heat losses, as shown in eq.2. For large $\dot{m}_a/A_c$ values there is a negligible temperature increase, as heat per unit of mass is small. The efficiency in this case would be high, as losses are small (low collector temperature), but no appreciable temperature increment is achieved, and thus there is no substantial relative humidity decrement. Therefore, the collector is useless. In the intermediate zone both the collector

efficiency and the temperature increase are relevant and intermediate.

The maximum drying capacity that can be obtained from such airflow is presented in Fig.3. In this graph the dimensionless variable presented in eq.6 is depicted, so the actual drying capacity also depends on irradiation and collector area.

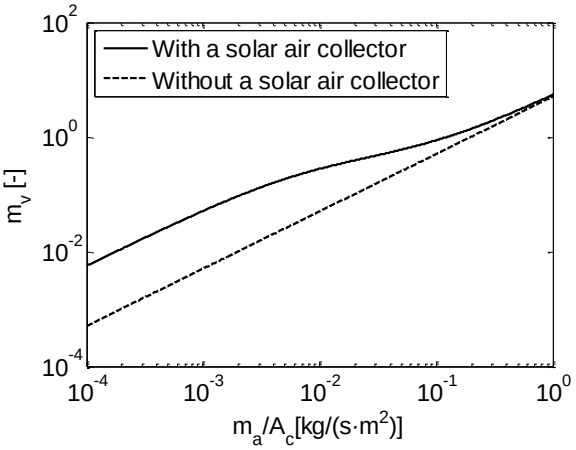

Fig.3. Maximum dimensionless vapour mass flow rate

Cases with and without the solar collector are shown for a wide range of air mass flow per unit of collector area. The case without collector (where the drying capacity is calculated assuming that airflow enters directly to the drying chamber and thus the drying process begins at ambient temperature) is depicted for comparison. Nevertheless, it may seem strange to plot this case with an abscise axis that includes the collector area, but this area appears in both axis (check eq.6), so both terms cancel.

The curves in Fig.3 show a proportional trend with the mass flow rate. Doubling the vapour mass rate can be obtained by doubling the air mass flow. In the case without collector this is the only effect. In the collector case, another effect is present, as a result of the temperature increase in the collector, and modifies the air mass flow effect. The same three regions observed in Fig.2 are shown here, as the temperature increase in the collector produces a specific humidity difference in the drying chamber between inlet chamber conditions and saturation. When the mass flow rate per unit of collector area is low, the use of the collector improves the drying capacity, as an appreciable temperature increase in the solar collector is obtained, and thus an increment in specific humidity can be achieved. The consequence is that the vapour mass flow rate is not proportional to the air mass flow rate in the 10^{-3}-10^{-1} kg/(s·m^2) range. Below 10^{-3} kg/(s·m^2), the effect of the collector is maintained, but the proportional effect of the air mass flow reappears. These two effects explain that most dryers work in this range. The first one is of special interest for forced convection dryers, as it produces an increase of the vapour mass rate that is not directly a consequence of increasing the airflow (and thus the fan power). The second effect is of lesser interest (as the airflow is small) and will be a field for natural convection dryers working with small airflows. When the mass flow is too large for the collector area, no temperature increment is achieved and the results with and without collector collapse.

B. Drying chamber performance

The previous results are presented for a wide range of air mass flow rates, but results for the drying process are calculated for a narrower range (air velocities between 0.2 and 1.7m/s, and $\dot{m}_a/A_c$ between 0.02 and 0.17 kg/(s·m^2)), and with some dimensions fixed (collector length and flow cross sections in both collector and drying chamber), as established in the previous section.

Figure 4 shows the evolution along the drying chamber of the temperatures and specific humidities that control the drying process (eq.8). Note that the tray disposition in the drying chamber is not defined in this work, and the calculations rely on the total length available for heat and mass transfer between the product and the airflow, regardless of the disposition (and as long as the correlations of eq.9 can be accepted).

Results are presented in dimensionless terms, and for an intermediate value of airflow velocity of 0.95m/s. As the airflow moves along the drying length its moisture content increases and its temperature decreases (as an adiabatic process has been assumed), approaching the wet bulb temperature. The surface temperature (and thus its specific humidity for saturated conditions) is

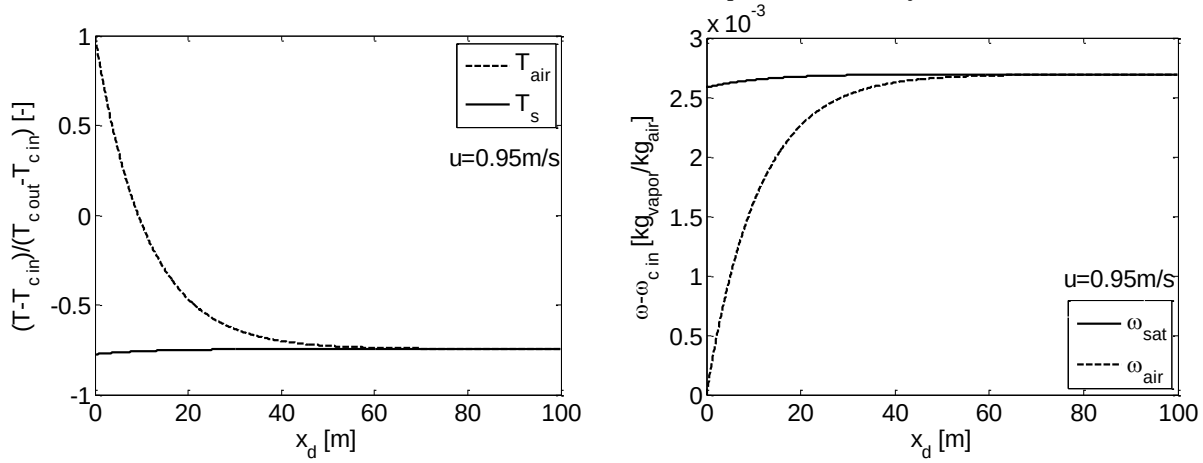

Fig.4. Surface and airflow temperatures and relative humidities along the drying chamber.

determined by the heat balance of eq.8. The results show an almost constant surface temperature. For large lengths, air and surface conditions merge and the drying process stops. Evidently enough, the local amount of vapour mass transferred from the surface to the airflow decreases along the chamber. That behaviour may provide with an economic criterion for the drying chamber dimensions.

The temperature graph shows the evolution of both the airflow and the surface temperatures. The dimensionless temperature parameter is the difference of these temperatures with ambient temperature compared to the temperature increment in the solar collector. Therefore, negative values represent temperatures lower than the ambient temperature. As the air flows along the dryer it losses heat, used to evaporate the water on the product surface, and thus its temperature decreases. The specific humidity evolution is presented as the increment in specific humidity of air from ambient conditions. Both graphs show that the airflow temperature and humidity change mainly in the first 20 meters, and reach saturation values around 40 meters for this specific configuration.

From the results of Fig.4, the vapour mass flow can be calculated using eq.7. It can be compared with the maximum vapour mass flow depicted in Fig.3, which is the drying capacity of the airflow to saturation and corresponds to the case for $L_d \to \infty$. An efficiency of the drying chamber can thus be defined in the form:

$$\eta_{dry} = \frac{\dot{m}_v(L_d)}{\dot{m}_v(L_d \to \infty)} \qquad (6)$$

The results for such efficiency as a function of the total drying length are presented in Fig.5 for different air velocities along the drying chamber.

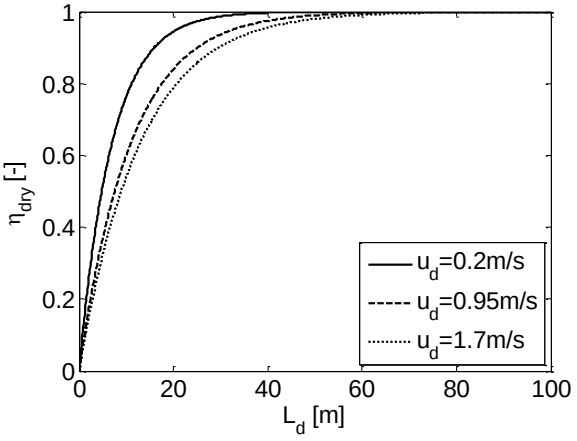

Fig.5. Drying efficiency of the drying chamber

Fig.5 shows that a decrease of the airflow velocity results in a reduction of the drying chamber dimensions, when maintaining the same efficiency. This is due to the dependence on the velocity of the mass and heat convection coefficients. Both coefficients, disregarding the minor effect of the variation of the Schmidt number (as the diffusion coefficient varies with temperature) are a function of $u^{0.71}$ (see eq.9). An increase of the velocity produces an increase of the mass flow rate, but a decrease ($\sim u^{-0.29}$) of the mass extracted per unit length ($\dot{m}_a/u$).

Nevertheless, the maximum vapour flow rate varies with the mass flow, as established in Fig.3. Combining the results on Fig.3 and Fig.5, the mass flow rate of vapour was obtained as a function of the air mass flow rate per unit of collector area, and for different lengths of the drying chamber. The results are shown in Fig.6. From the dimensionless variable depicted in Fig.6, the dimensional vapour mass flow rate can be obtained using eq.6.

The solid line represents the maximum vapour mass flow previously represented in Fig.3, but for the range of study here, which is $2 \cdot 10^{-2}$ to $2 \cdot 10^{-1}$ kg/(s·m^2). Note that the axes scale of the figure is linear in both axes, not log-log as was the case of the previous graph. The range represented is that where the vapour mass rate is defined by the combined effect of the air mass flow and the effect of the collector in increasing its available humidity increment. Thus the vapour mass rate is not proportional to the air mass flow, but a factor 10 increase of the air mass flow results in an approximately factor 3 increase of the vapour mass rate. This is the result, as explained previously, of the decaying effect of the collector. An increase of the collector area would be a solution in such cases. The three dotted-dashed lines in Figure 6 represent the results for drying chambers of different dimensions. It is shown that the effect of the air mass flow rate diminish for diminishing lengths. For a 5 m drying chamber, the effect of the air mass flow is rather small, a factor 10 increase of the air mass flow producing a factor 2 increase of the vapour mass rate. This is produced by an important reduction of the residence time of the air in the drying chamber. For large air mass flows and small drying chambers, this will result of the airflow leaving the chamber unsaturated, thus reducing the drying efficiency.

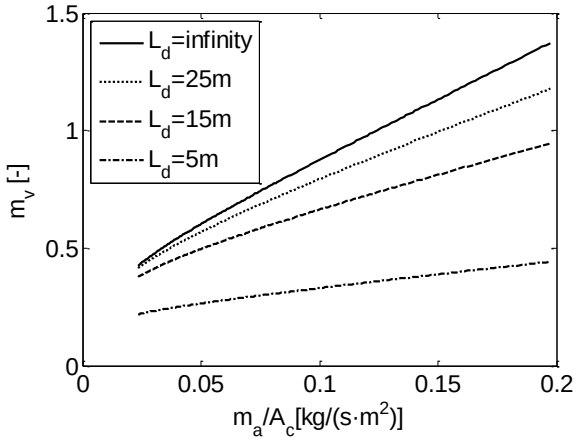

Fig.6. Vapour mass flow rate (dimensionless) as a function of design parameters

Therefore, a proper definition of the collector and drying chamber dimensions (collector area and chamber length) as a function of the available air mass flow is customary for a proper design of the dryer.

5. Conclusions

This work presents a model of the main processes occurring in an indirect solar dryer for batch drying. The collector performance and the drying chamber performance, both separately and jointly, have been analysed, studying the influence of the design parameters. These design parameters are the airflow velocity and the dimensions of the solar collector and the drying chamber.

The collector performance depends on the air mass flow rate per unit of collector area. The collector is shown to be useful for a range of air mass flow rates per unit of collector area between 0,01 $\mathrm{kg/(m^2 s)}$ and 1 $\mathrm{kg/(m^2 s)}$. Lower values are burdened by very low collector efficiencies, as high temperatures are reached and thus, losses are important. Larger values show that the collector is unnecessary, as all the heat is carried away by the airflow with a negligible increase of its temperature. The collector performance defines the drying capacity of the airflow in that region, diminishing the effect of the air mass flow, which is proportional to the vapour mass rate in the zones where the collector is not well design. This drying capacity would be reached or not depending on the fulfilment of the drying process occurring in the drying chamber. This process is affected, besides the temperature, by the airflow velocity and the dimensions of the drying chamber.

The results in the drying chamber, obtained for a particular geometrical configuration, show the evolution of the drying process and the effect of the chamber length (along the drying process). Convection coefficients for mass and heat transfer acquire larger values as the airflow velocity increases. However, a high airflow velocity yields a low residence time in the drying chamber, a factor that could result in low drying efficiency, as the airflow would not have time to saturate, losing part of its drying capacity.

Air mass flow rate, collector area and drying chamber length are the key parameters in the design of an indirect solar dryer. The air mass flow rate is the more relevant factor, but it adds to the cost of the dryer (fan and fan power) or is low (natural convection dryers). A proper design of the collector, with a suitable air mass flow to collector area rate (in the 10^{-3}-10^{-1} kg/s/m^2 range) would allow to higher drying capacities for lower air mass flows. The drying chamber length and geometry should also be selected as a function of the air mass flow rate; a small length may result in low drying efficiency and a waste of the drying capacity of the airflow; a large length resulting in useless economical costs to the drying assembly.

Nomenclature

A_c Solar collector area [m^2]
A_d Drying surface area. [m^2]
C_{p_a} Air specific heat [J/(kg·K)]
C_{p_v} Vapour specific heat [J/(kg·K)]
F_R Heat removal factor [-]
h_c Heat convection coefficient [W/(m^{2}K)]
h_{fg} Vaporization enthalpy [J/kg]
h_g Enthalpy of saturated vapor at 0ºC [J/kg]
I_T Solar irradiance [W/m^2]
K Convective mass transfer coefficient. [kg/(s·m^2)]
L Solar collector length [m]
L_d Drying chamber length [m]
$\dot{m}_a$ Air mass flow [kg/s]
$\dot{m}_v$ Vapour mass flow [kg/s]
P_{atm} Atmospheric pressure [Pa]
Pr Prandtl number [-]
P_{ref} Reference saturation pressure at $\mathrm{T_{ref}} = 30$ºC [Pa]
Re_D Reynolds based on hydraulic diameter [-]
R_g Gas constant for vapour [J/(kg·K)]
s Solar collector thickness [m]
s_d Space between trays [m]
Sc Schmidt number [-]
T_0 Reference temperature 0ºC [K]
$T_{c\,in}$ Temperature of air at the collector outlet [K]
$T_{c\,out}$ Temperature of air at the collector outlet [K]
$T_{o\,sat}$ Temperature of saturated air at the drying chamber outlet [K]
T_{ref} Reference temperature 30ºC [K]
T_s Temperature of the surface of the product [K]
T_∞ Temperature of air in the drying chamber [K]
u Airflow velocity in the collector [m/s]
u_d Airflow velocity in the drying chamber [m/s]
x_d Drying chamber longitudinal coordinate [m]
W Solar collector width [m]
W_d Solar collector width [m]
α Absorptance [-]
η Solar collector efficiency [-]
η_{dry} Drying efficiency of the drying chamber [-]
$\omega_{c\,in}$ Specific humidity of air at the solar collector inlet [$\mathrm{kg_{vapour}/kg_{air}}$]
$\omega_{o,sat}$ Specific humidity of saturated air at the drying chamber outlet [$\mathrm{kg_{vapour}/kg_{air}}$]
ω_{sat} Specific humidity for saturation conditions at the surface temperature [$\mathrm{kg_{vapour}/kg_{air}}$]
ω_∞ Specific humidity of saturated air at the drying chamber outlet [$\mathrm{kg_{vapour}/kg_{air}}$]
ρ Air density [kg/m^3]
τ Transmittance [-]

References

[1] Mujumdar, A. S. (Editor), 2007. Handbook of industrial drying, 3rd Edition. CRC Press.

[2] Duffie, J.A., Beckman W.A., 2006. "Solar engineering of thermal processes". 3rd Edition. John Wiley & Sons

[3] Treybal R.E., 1987 "Mass-Transfer Operations". 3rd Edition. McGraw Hill

[4] Bolaji B.O., 2005. Development and performance evaluation of a box type absorber solar air collector for crop drying. Journal of food technology, 3. 595-600.

[5] Karim, M.A., Hawlader, M.N.A., 2004. Development of solar air collector for drying applications. Renewable Energy, 32, 1645-1660.

[6] Pangavhane, D.R., Sawhnei, R.L., Sharsavadia, P.N., 2002. Design, development and performance testing of a new natural convection solar dryer. Energy, 27, 579-590.

[7] Madhlopa, A., Jones, S.A., Saka, J.D.K., 2002. A solar air heater with composite absorber system for food dehydration. Renewable Energy, 27, 27-37